Arab J Sci Eng (2017) 42:4597–4604
DOI 10.1007/s13369-017-2585-0

RESEARCH ARTICLE - MECHANICAL ENGINEERING

Microstructure and Wear Properties of Laser-Cladded cBN/Ti_3Al on Pure Titanium

K. K. Sobiyi[1] · **E. T. Akinlabi**[1]

Received: 20 October 2016 / Accepted: 8 May 2017 / Published online: 20 May 2017

Abstract In order to improve the tribological properties of titanium alloys at high temperature, the possibility of producing Ti_3Al intermetallic with the addition of ceramic (cBN) coatings on titanium substrate using laser technique cladding was investigated. cBN is generally known for its high hot hardness, wear resistance and chemical stability. Laser cladding is an emerging material processing technique which is an efficient and cost-effective technique for improving the surface properties of general metallic materials. This paper presents the effects of laser cladding on the phase combination, microstructure, hardness and wear resistance of titanium aluminide/cBN IMC composites at different variations in quantity of cBN in the composite. Optical microscopy, X-ray diffraction and scanning electron microscopy with EDX were used for characterising the microstructure of the coating. In addition, the composite coating was subjected to wear testing using the ball-on-disc, friction and wear apparatus. The XRD results revealed phases with small cBN, Ti_2N and TiB_2 peaks in addition to the rich γ-Ti, $\alpha 2$-Ti_3Al and TiAl intermetallics phases in the coatings after cladding process, whereas the microstructure of the cBN cladded layer contained partially melted cBN grains evenly dispersed within the laths of alpha Widmanstätten phase in the form of dendrites, precipitate of α_2-Ti_3Al and spherical-shaped pure titanium. The effect of the addition of cBN into Ti_3Al alloy at increasing weight percentages showed an improvement in the hardness and wear resistance of the coatings. The increase is attributed to reacted boron nitrides particles with titanium, being distributed uniformly in the intermetallic matrix.

Keywords Titanium · Intermetallics · Laser cladding · cBN · Wear

1 Introduction

Laser cladding is an efficient, cost-effective and environmentally friendly surface modification technology, which has been extensively used for providing thermal barrier (TBC) coatings for engineering components [1]. During laser cladding process, a high-power laser beam is utilised to locally melt the coating materials and a thin surface layer of a substrate material; thus, a new layer of material with desired properties is formed after solidification [2].

Titanium alloys are widely used in the aerospace, chemical and medical industries owing to the excellent combinations of specific mechanical properties and corrosion resistance. However, the poor tribological properties of these alloys have limited its use in severe wear applications [1,3,4]. Single and multiple ceramic materials are commonly used as coatings in improving the surface properties of titanium. However, these materials are highly susceptible to cracking, thus restricting their industrial applications [5,6]. TiAl intermetallics are normally used as a binding phase between titanium alloys matrix and the ceramic reinforced phase to reduce the cracking and residual stress associated with ceramic coatings [6]. Furthermore, TiAl present several advantages such as low density, high melting point, good structural stability, high strength at elevated temperature, good corrosion resistance, high elastic modulus and good creep resistance [2,7,8]. cBN is found to be a suitable material for improving wear resistance of metal

✉ K. K. Sobiyi
kk_sob@yahoo.com

[1] Department of Mechanical Engineering Science, University of Johannesburg, Auckland Park Campus, Johannesburg 2006, South Africa

composites because of its high hardness, wear resistance and excellent chemical stability at high temperatures [9–11].

Laser cladding of combination of Ti, Al and ceramics such as Ti–Al–B_4C, TiN, TiC and SiC reinforced Ti_3Al IMC coatings on titanium and its alloys has been extensively studied [12–14]. The authors reported improvement in the hardness and wear resistance of the resulting surface after laser cladding. Selvan et al. [15] investigated CO_2 laser alloying of pre-placed BN coating on Ti–6Al–4V alloy. They observed the formation of titanium nitride and titanium boride in the coating, and hardness up to 1700 was recorded. Although the effects of ceramic addition to TiAl intermetallics have been reported, there are no reports on laser cladding of the combination of cBN with Ti_3Al intermetallics.

This study presents the effects of laser cladding on the phase combination, microstructure, hardness and wear resistance of titanium aluminide/cBN IMC composites at different variations in quantity of cBN in the composite.

2 Experimental Procedure

Commercial cBN powder (average particle size of 100 μm), titanium powder (average particle size of 60 μm) and aluminium powder (average particle size of 200 μm) were cladded on the surface of 99.6% pure titanium substrate (75 mm × 75 mm). Before the laser cladding experiments, the titanium and aluminium powders were premixed in nominal chemical constituents (atomic fraction, %) of 70Ti–30Al ratio of 70:30, respectively, in order to produce Ti_3Al intermetallics alloy, through the reaction of Ti and Al during the laser cladding process. cBN powders were fed in volume ratio of 5, 10 and 15% using a dual powder feeding system hoppers. Before the cladding process, the substrate was sand-blasted and then rinsed in acetone to clean the surface.

Laser cladding was carried out by a Kuka robot, 4.4 KW Nd-YAG laser machine. The deposition was performed using a laser focal length of 195 mm and beam spot size of 4 mm. Laser power and scanning speed were kept constant at 1500 W and 1.0 m/min, respectively. These parameters were fixed at optimum parameters, based on previous experiments in order to produce claddings with good metallurgical bonding. The cladding powders were shielded by argon gas at a flow rate of 2 l/min with the oxygen level being kept in the 10 ppm level (to avoid oxidation of the substrate and as well as the cladded layer, through reaction with oxygen) using a glove box.

X-ray diffraction analysis was performed using Bruker D8 Venture Photon CMOS. Microscopic examination was performed by means of an optical microscope (Olympus BX51 M) and scanning electron microscope (ZEISS) equipped with EDAX Oxford energy-dispersive spectroscopy (EDS). Microhardness was measured using a Vickers microhardness testing machine (EMCOTEST®). The test load of 500 g/f with a dwell time of 10 s was used. Ten indentations were applied per sample, and the average diagonal values of the samples were recorded.

Dry sliding wear test was performed on the cladded surfaces using the ball-on-disc mode on friction and wear apparatus. The sample was preloaded with counterbody balls made of tungsten carbide with diameter of 10 mm. The applied load was 25 N with stroke length of 2 mm, sliding distance of 1000 m and sliding time of 1000 s at a frequency of 5 Hz. The coefficient of friction was plotted against time for 1000 s and recorded by the computer attached to the tribometer. Wear resistance testing was performed according to ASTM G133-05 standards [16]. Wear volume loss of the substrate and coating was calculated from Eq. (1) [16,17].

$$V_{\text{total}} = V_A + V_B = L\left\{r^2\sin^{-1}\left(\frac{W}{2r}\right) - \frac{W}{2}\left(r^2 - \frac{W^2}{4}\right)^{1/2}\right\} + \frac{\pi}{3}\left\{2r^3 - 2r^2\left(r^2 - \frac{W^2}{4}\right)^{1/2} - \frac{W^2}{4}\left(r^2 - \frac{W^2}{4}\right)^{1/2}\right\} \quad (1)$$

where 'r' is the radius of the sphere used, 'w' the wear track width and 'L' the length of the wear track. The micrograph of the wear surface morphology and wear debris of the coatings was observed under the SEM.

3 Results and Discussion

3.1 Microstructure Characterisation

The X-ray diffraction pattern of the cBN/Ti_3Al composite coatings on the pure titanium substrate is shown in Fig. 1. The intermetallic coating with 0 vol% cBN has a phase composite consisting of mainly $\alpha 2$-Ti_3Al intermetallic and γ-Ti solid solution. During the reaction between the individual elements of Ti and Al, it is considered that the ordered stoichiometric phase of $\alpha 2$-Ti_3Al is preferred to form. However, the high peaks of pure titanium (γ-Ti) in the coating showed the presence of incomplete reaction of the titanium with the aluminium powders.

The addition of cBN powders in the coatings showed phases with small cBN, Ti_2N and TiB_2 peaks in addition to the rich γ-Ti, $\alpha 2$-Ti_3Al and TiAl intermetallics phases. The reaction of pure titanium with the boron nitride leads to the formation of Ti_2N and TiB_2 compound in the coatings. The degree of formation of Ti_2N and TiB_2 compound during the exothermic reaction between Ti and BN could be described as follows:

$$[\text{Ti}]_{(l)} + \text{BN}_{(s)} = \text{TiN}_{(s)} + [\text{B}]_{(s)} \quad (2)$$

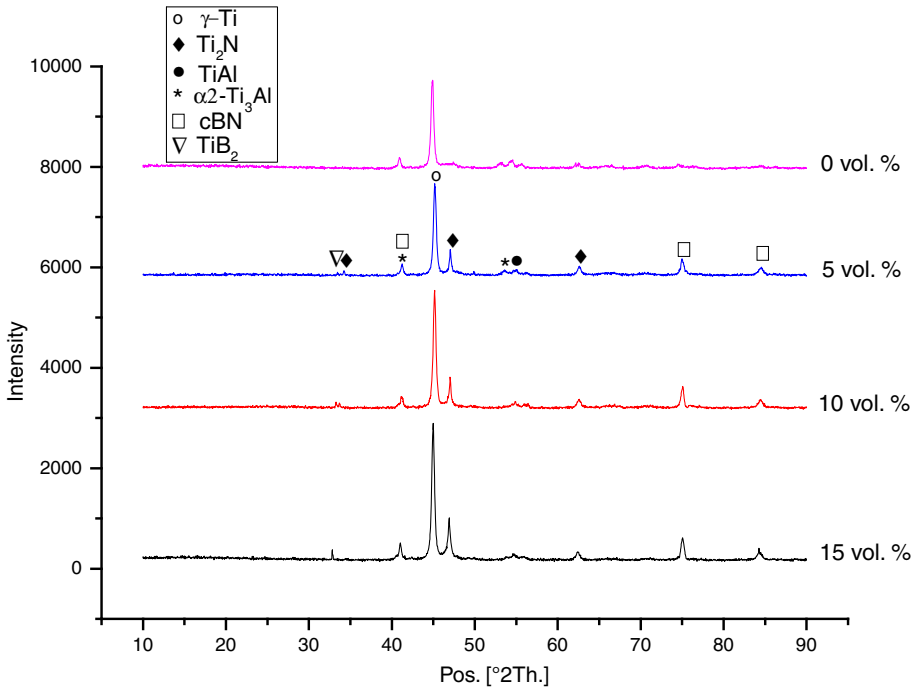

Fig. 1 XRD pattern of the composite coatings on the pure titanium substrate

$$[\mathrm{Ti}]_{(l)} + 2\mathrm{BN}_{(s)} = \mathrm{TiB}_{2(s)} + \mathrm{N}_{2(g)} \quad (3)$$

$$[\mathrm{Ti}]_{(l)} + \mathrm{TiN}_{(s)} = \mathrm{Ti_2N}_{(s)} \quad (4)$$

$$[\mathrm{Ti}]_{(l)} + 2[\mathrm{B}]_{(s)} = \mathrm{TiB}_{2(s)} \quad (5)$$

In the reaction described above, the dominating factor in the formation of Ti–N and Ti–B compounds is titanium.

The diffraction intensities of cBN, Ti_2N and TiB_2 peaks, however, increases as the percentages and the amount of reaction product increase in the composites coatings. A more noticeable broader intensity of the Ti_2N peaks is visible at increasing cBN content from 10 to 15% due to the dissolution of nitrogen atoms in the hcp Ti lattice; the broader peaks indicate a more amorphous state of the titanium nitride.

Figure 2a–d shows the scanning electron micrograph (SEM) of the deposits on the substrate after laser cladding of the titanium aluminide powders. The coatings on all the samples produced were observed to be metallurgically bonded with the substrates and the microstructure relatively homogeneous. The microstructure of the intermetallic coatings with 0 vol% boron nitride (cBN) content appeared to be free of cracks, but few pores are visible within the coatings. However, the microstructure of the samples containing 15 vol% cBN in the composite coatings has few cracks (see Fig. 2e), usually towards the end of the heat-affected zone. The cracks are due to the surface tension gradient and high convective flow between the molten intermetallic liquid and the partially molten cBN powder particles during the rapid solidification of the coatings during laser cladding, thus leading to stresses in the coatings [15,18]. It can be noted that the number of partially melted cBN particles within the microstructure is more as compared at optimum cBN composition.

In addition, the titanium aluminide coatings with 5, 10 and 15 vol% cBN content have few visible pores within the microstructure. The pores increase with the increase in the cBN content in the deposits. The pores are caused by the gas [possibly N_2 that escaped during the exothermic reaction of Ti with BN as indicated in Eq. (2)], produced from the in situ synthesised TiB_2/cBN/Ti/Ti_2N/Ti_3Al IMC coating, entrapped within the molten pool as a result of large viscosity induced by the material particles during the laser cladding process [3,17,19].

The microstructure of the layer cladded with 0 vol% cBN consisted mainly of Widmanstätten alpha phase in beta matrix (see Fig. 2a). The microstructure of the titanium aluminium cladded layer with 5, 10 and 15 vol% cBN content as shown in Fig. 2b–d, contained cBN grains (partially reacted with titanium particle) evenly dispersed within the laths of alpha Widmanstätten phase in form of dendrites and as well as precipitate of α_2-Ti_3Al, and spherical-shaped pure titanium. As the percentage of the cBN increases in the cladded layer, the structure of the cBN grains is more defined. Partially melted cBN particles dispersed within the cladded layer was observed mostly visible in the 15% cBN cladded layer.

Figure 3a shows the microstructure of the intermetallic coatings with 15 vol% boron nitride (cBN), showing the deposit zone, bond zone, heat-affected zone and the substrate. Partially reacted cBN particles with fine equiaxed precipi-

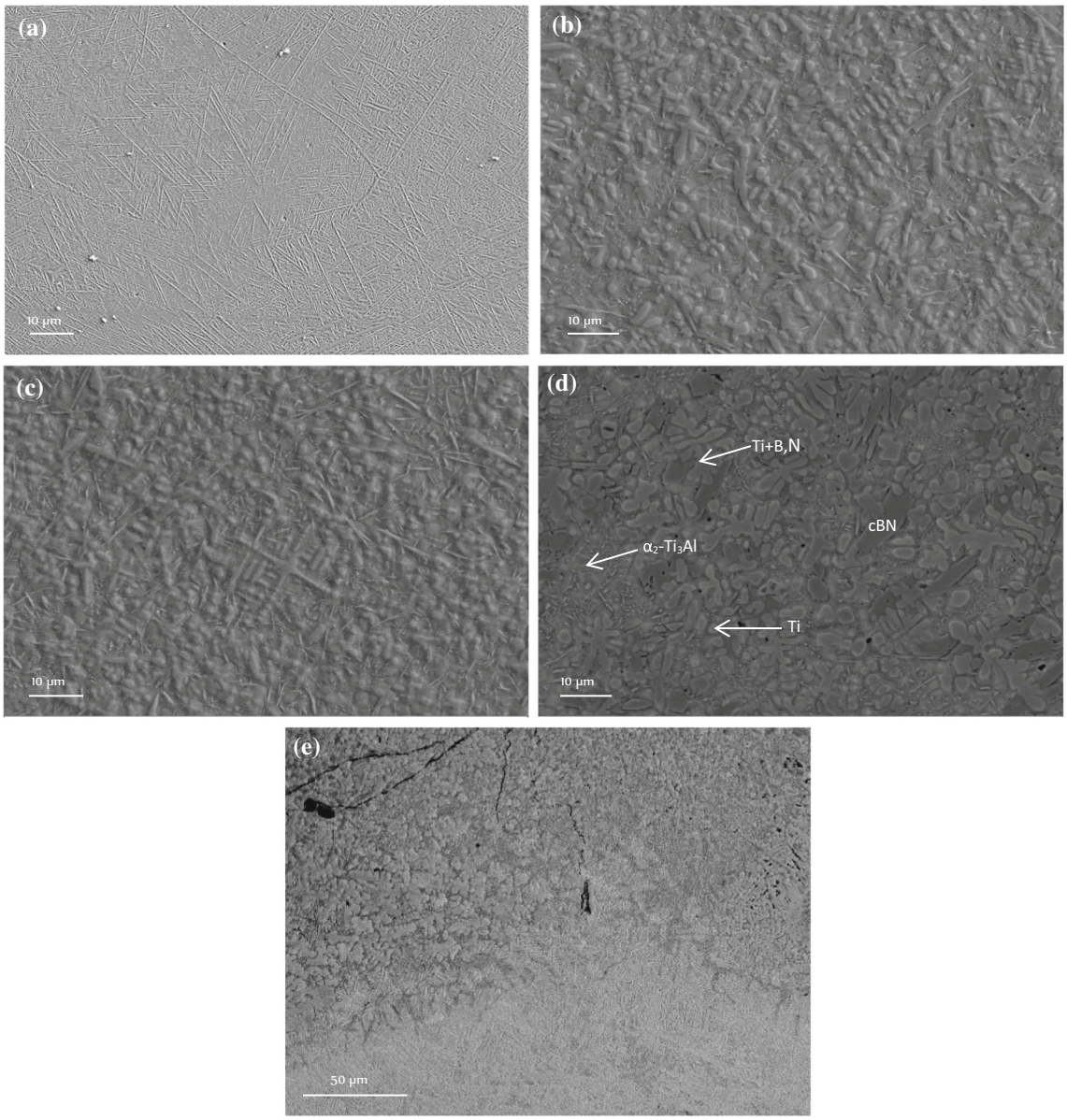

Fig. 2 Microstructure of the laser-cladded composite coatings on the pure titanium substrate at varying quantity of cBN **a** 0 vol%, **b** 5 vol%, **c** 10 vol%, **d** 15 vol% and **e** crack formation (15 vol%)

tates of α_2-Ti_3Al were commonly observed in the deposit zone (Fig. 3b). The bond zone and heat-affected zone near the substrate contained acicular martensite with distributed lamellae phase (phase composition of 13.9 at.% Al and 86.1 at.% Ti), while the substrate contained recrystallised alpha grains, and particles of beta stabilised by impurities.

The microstructure of the titanium aluminide intermetallic coating with 15 vol% cBN content at the deposit zone (higher magnification) is shown in Fig. 3b. The figure shows a clearer representation of the morphological features of the deposit zone. The results of the EDS analysis of the phases with different morphological features are presented in Table 1. The darker dendritic phase showed a BN-rich region, whereas the composition of BN is much lower in the lighter dendritic phase. The white needle-like particles observed in the alloyed layer is composed mainly of α_2-Ti_3Al and TiB_2. The spherical particles contain mainly titanium, and the dendritic structure consists mainly of titanium nitride in atomic ratio approximately 2:1, identified as Ti_2Ni, similarly observed by [15]. These elements were also confirmed with the XRD traces as shown in Fig. 1.

In summary, the microstructure of the cladded IMC coatings showed different morphological features from the surface (deposit zone) to the substrate with refined cBN grain particles as the vol% cBN content increases in the deposits. The formation of hard ceramic compounds in situ synthe-

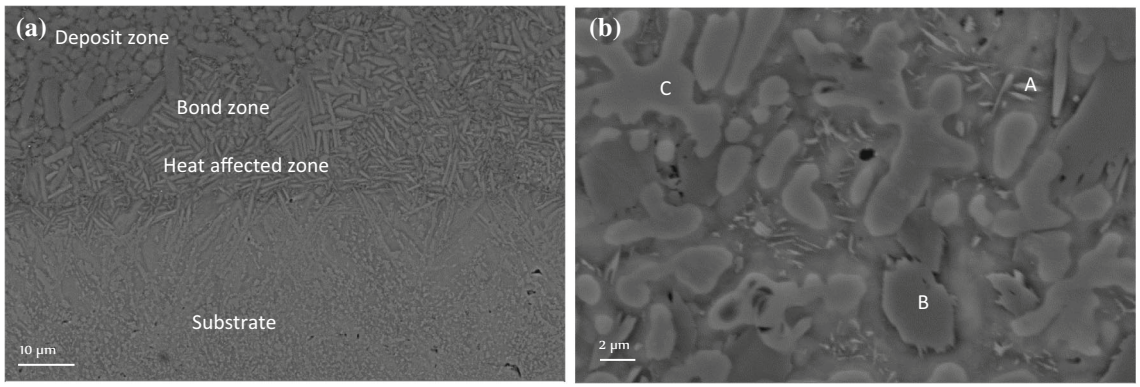

Fig. 3 Microstructure of titanium aluminide intermetallic coating with 15% cBN content. **a** Interface. **b** Deposit zone at 10,000×

Table 1 Chemical composition (at.%) of the phases formed on the 15 vol% cBN content coating

Analysis zone	Ti	Al	BN
A	79.45	21.55	–
B	62.27	0.90	36.83
C	99.49	0.51	–

sised and Ti–Al intermetallic was more predominant in the coatings cladded with higher vol% cBN content.

3.2 Microhardness

Figure 4 shows the graphical profile of the Vickers microhardness measured across the depth direction of the laser-cladded sample with layer of titanium aluminide intermetallic with 0 vol% cBN from top to bottom. It was observed that the microhardness decreases towards the substrate along the profile. The hardness of the deposit zone was higher than that of the substrate as shown in Fig. 4. The average hardness at the deposit zone (coating) is approximately 430 $HV_{0.5}$ compared to the pure titanium substrate of 190 $HV_{0.5}$. The higher hardness at the deposit zone is attributed to the presence of homogeneous dispersion of TiAl and α_2-Ti_3Al phases within the coating [19].

Similarly, high hardness that is slightly lower than that of the deposit zone was observed at the transition between the deposit and heat-affected zone. This hardness can be attributed to possibly better crystallisation of the grains at this zone and also the lower heat experienced at the lateral inner part of the substrate [20].

Figure 5 presents the average Vickers microhardness of the coatings of the samples with 0, 5, 10 and 15 vol% cBN content. The hardness increases with an increase in the percentage of cBN addition to the cladded layer. The average hardness for the 0, 5, 10 and 15 vol% cBN content is 430 $HV_{0.5}$, 790 $HV_{0.5}$, 940 $HV_{0.5}$ and 1024 $HV_{0.5}$, respectively.

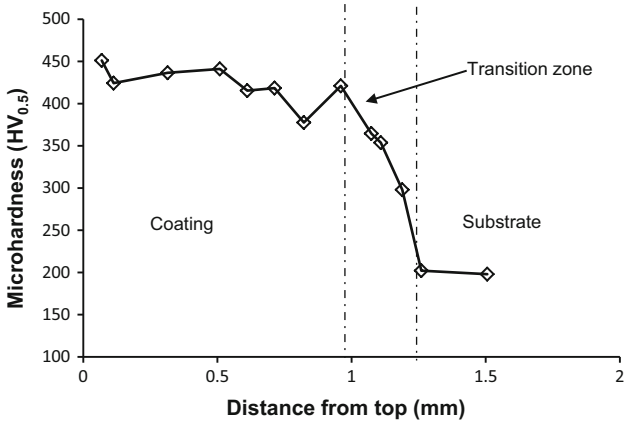

Fig. 4 Microhardness profile of coatings containing 0% cBN content

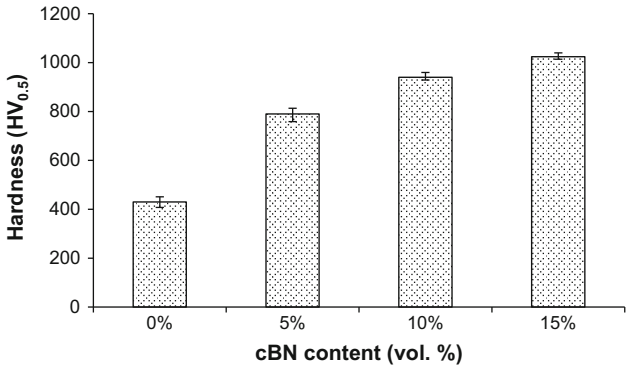

Fig. 5 Hardness of the composite coatings cladded on the pure titanium substrate

The small addition of cBN up to 5 vol% to the titanium aluminide in the coating increased the hardness to almost twice the value. The increase in the hardness at the cladded layer with increasing cBN content is due to the presence of hard cBN particles (precipitates of titanium nitride and titanium boride) dispersed within the TiAl and α_2-Ti_3Al phases.

3.3 Wear Resistance Behaviour

Figure 6 presents the results of the experimental coefficient of friction of the dry sliding wear resistance tests plotted against time for the coatings cladded on the pure titanium substrate. The coefficient of friction of the coatings was generally observed to increase slightly with the increase in time. A high coefficient of friction was recorded for the coating containing 0 vol% cBN content. The coefficient of friction reduces as the cBN content is increased from 5, 10 and 15 vol%, respectively. This indicates that the coatings with higher percentage of cBN exhibited better frictional coefficient under the normal load. At optimum composition of cBN content (15 vol%), it can be seen that the coefficient of friction reduces with time. This can be attributed possibly to the low penetration of the sliding ball and the presence of more partially melted cBN particles within the matrix of the titanium alloy causing ore resistance to the tungsten carbide counterbody. The hard cBN particles embedded in the softer titanium aluminide matrix help increase the sliding resistance, thus decreasing the value of the frictional coefficient. The presence of the cBN improved the wear resistance performance of the substrate.

Figure 7 shows the wear volume of the pure titanium substrate and the titanium aluminium/cBN IMC coatings with different volume fractions of cBN sliding against WC ball under 25 N normal load. The volume of material removed from the substrate decreased by 2.3 times with the application of titanium aluminide as a coating on the substrate. In this light, less material was removed from the coating with addition of cBN particle to the titanium aluminide. The volume of material removed decreased by 3.2, 4.2 and 8.8 times for 5, 10 and 15 vol% addition of cBN to the titanium aluminide coating, respectively, as compared to pure Ti substrate. The coating with mainly Ti_3Al (0 vol% cBN) had poor wear resistance compared to the titanium aluminium/cBN IMC coatings containing 5, 10 and 15 vol% cBN content. The poor wear resistance results from its high coefficient of friction and higher chemical affinity with the WC balls [21]. As observed, the wear volume of the cBN/ Ti_3Al IMC coatings decreases with the increase in the volume fraction of cBN content in the coatings. The coating with 15 vol% cBN had the highest wear resistance.

The SEM micrograph of the worn cBN/ Ti_3Al IMC coatings with different volume fractions of cBN powder after sliding under the WC ball is shown in Fig. 8. All the coatings showed loose debris on the worn surfaces containing W, C and O elements indicating the occurrence of oxidation wear [22]. For the Ti_3Al coating, the wear mechanism observed is mainly abrasive wear feature as evidenced by grooves on the worn surface. The wear tracks comprised abraded regions with continuous microgrooves parallel to the direction of sliding.

The cBN/Ti_3Al IMC coatings with different fractions of cBN powders showed different wear mechanism. For the coatings with 5 vol% cBN the worn surface showed evidence of plastic deformation as well as abrasive wear features, whereas the worn surface of coatings with higher cBN content is mostly covered with pits and transferred layer without the features of microgrooves, indicating a combination of severe plastic deformation, oxidation and adhesive wear (observed as adhesive craters on the wear surface) features. Evidence of wear debris consisting of small flakes and tiny particles was observed on the worn surfaces (see Fig. 8). The presence of plastic deformation in the sliding contact area is responsible for the surface morphology [23]. Evidence of pull out of harder phases (partially melted particles of cBN powder) was also observed on the worn surfaces of the coatings with 10 and 15 vol% cBN. The feature was more common with the coating with 15 vol% cBN. In addition, irregular wear debris and accumulated fine particles, micropatches and delaminated scars on the worn tracks were observed within the worn zone.

The hard ceramic reinforced phases of TiB_2-Ti_2N in the cBN/Ti_3Al IMC coatings (5, 10, 15 vol% cBN) is responsible

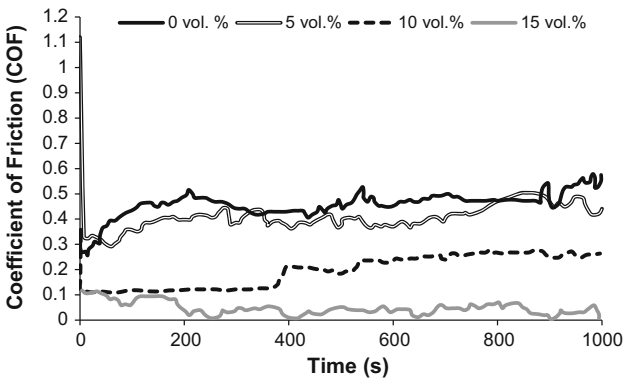

Fig. 6 COF against time during dry sliding wear resistance tests of the titanium aluminium/cBN IMC coatings

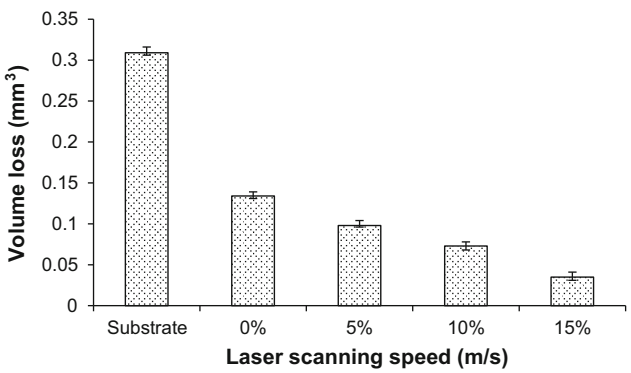

Fig. 7 Wear volume loss for the titanium aluminium/cBN IMC coatings

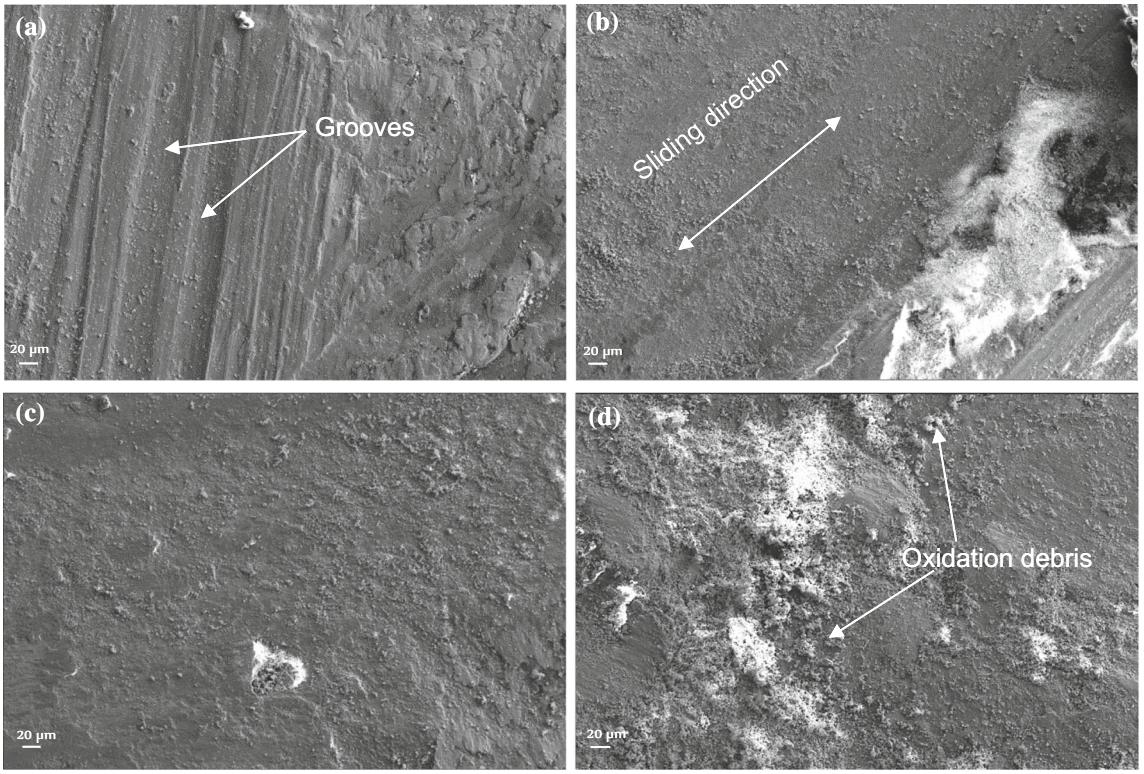

Fig. 8 SEM micrograph of the worn titanium aluminium/cBN IMC coatings **a** 0 vol%, **b** 5 vol%, **c** 10 vol%, **d** 15 vol%

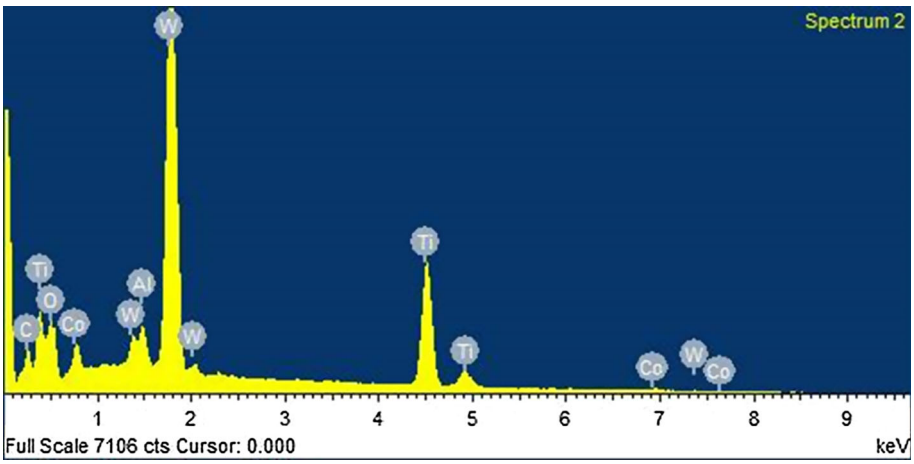

Fig. 9 EDS point analysis of wear debris

for the improvement in the wear resistance of these coatings by withstanding the external load applied by the sliding ball on the surfaces [24].

The EDS point analysis of the debris on the surface of the coatings containing 15 vol% cBN is shown in Fig. 9. The analysis showed the presence of elemental oxygen, aluminium, tungsten (originated from the contacting surfaces of the tungsten carbide counterpart), and titanium in atomic weight percentages of 27.3, 2.4, 34.3 and 14.9% respectively, leading to possible formation of titanium oxides and aluminium oxides. The presence of oxygen confirms the considerable oxidation experienced at the contacting surfaces by the coatings and the counterbody.

4 Conclusion

The study investigated the microstructure and wear resistance behaviour of laser-cladded cBN/Ti_3Al composites on pure titanium substrate by varying the quantity of cBN in the composite. The following conclusions can be drawn.

The laser-cladded surfaces showed few pores and cracks which increased with the increase in the addition of boron nitride to the titanium aluminide intermetallic coating.

The coatings produced the formation of hard intermetallic compounds of titanium aluminide, titanium nitride and titanium boride as confirmed with XRD and EDS analysis.

The results obtained through microstructure of the intermetallic coatings with varying percentage of boron nitride (cBN) revealed that dendritic structure consists mainly of titanium nitride, white needle-like particles of α_2-Ti_3Al and TiB_2 and spherical particles of titanium.

Microhardness results showed that the hardness increases with an increase in the percentage of cBN addition to the cladded layer. The precipitates of titanium nitride and titanium boride as well as partially melted cBN were responsible for the increase in hardness of the cladded layer.

The results of the wear tests indicates that the wear volume of material removed from the surface of the substrate is higher than the wear volume of material removed from the deposit surface. The coefficient of friction of substrate was observed to be higher for 0 vol% cBN as compared to the 5, 10, 15 vol% cBN cladded layer. This is as a result of the hard ceramic reinforcement phases of cBN, Ti_2N and TiB_2 formed during the laser cladding process. The addition of cBN to the titanium aluminide improved the wear properties of the alloyed cladded layer.

Thus, it can be concluded that improvement in the wear resistance, corrosion resistance, load-bearing capability and high temperature stability can be attained from the hardness level of the ceramic TiN and TiB phases formed during the laser cladding of pure Ti substrate surface. This makes the material more applicable in the aircraft propulsion systems and automotive industries.

Acknowledgements The authors would like to thank Tshwane University of Technology and CSIR National laser centre for allowing to use their test equipment.

References

1. Graf, B.; Gumenyuk, A.; Rethmeier, M.: Laser metal deposition as repair technology for stainless steel and titanium alloys. Phys. Procedia **39**, 376–381 (2012)
2. Guo, B.; Zhou, J.; Zhang, S.; Zhou, H.; Pu, Y.; Chen, J.: Phase composition and tribological properties of Ti–Al coatings produced on pure Ti by laser cladding. Appl. Surf. Sci. **253**, 9301–9310 (2007)
3. Tian, Y.S.; Chen, C.Z.; Li, S.T.; Huo, Q.H.: Research progress on laser surface modification of titanium alloys. Appl. Surf. Sci. **242**, 177–184 (2005)
4. Li, G.J.; Li, J.; Luo, X.: Effects of post-heat treatment on microstructure and properties of laser cladded composite coatings on titanium alloy substrate. Opt. Laser Technol. **65**, 66–75 (2015)
5. Zhong, M.; Liu, W.: Laser surface cladding: the state of the art and challenges. Proc. Inst. Mech. Eng. C: J. Mech. Eng. Sci. **224**, 1041–1060 (2010)
6. Weng, F.; Chen, C.; Yu, H.: Research status of laser cladding on titanium and its alloys: a review. Mater. Des. **58**, 412–425 (2014)
7. Cárcel, B.; Serrano, A.; Zambrano, J.; Amigó, V.; Cárcel, A.C.: Laser cladding of TiAl intermetallic alloy on Ti6Al4V. Process optimization and properties. Phys. Procedia **56**, 284–293 (2014)
8. Ramadoss, R.; Kumar, N.; Dash, S.; Arivuoli, D.; Tyagi, A.K.: Tribilogical properties of γ-TiAl alloy sliding with various counterbodies. Indian J. Eng. Mater. Sci. **21**, 473–476 (2014)
9. Poulachon, G.; Bandyopadhyay, G.P.; Jawahir, I.S.; Pheulpin, S.; Seguin, E.: Wear behaviour of cBN tools while turning various hardened steels. Wear **256**, 302–310 (2004)
10. Sobiyi, K.; Sigalas, I.: Chip formation characterisation and TEM investigation of worn PcBN tool during hard turning. Mach. Sci. Technol. **19**, 479–498 (2015)
11. Sobiyi, K.; Sigalas, I.: High speed machining of martensitic stainless steel using PcBN. J. Superhard Mater. **38**, 34–39 (2016)
12. Pu, Y.; Guo, B.; Zhou, J.; Zhang, S.; Zhou, H.; Chen, J.: Microstructure and tribological properties of in situ synthesized TiC, TiN, and SiC reinforced Ti3Al intermetallic matrix composite coatings on pure Ti by laser cladding. Appl. Surf. Sci. **255**, 2697–2703 (2008)
13. Guo, B.; Zhou, J.; Zhang, S.; Zhou, H.; Chen, J.: Microstructure and tribological properties of in situ synthesized TiN/Ti3Al intermetallic matrix composite coatings on titanium by laser cladding and laser nitriding. Mater. Sci. Eng. A **480**, 404–410 (2008)
14. Li, J.N.; Chen, C.Z.; Cuia, B.B.; Squartini, T.: Surface modification of titanium alloy with the Ti3Al + TiB2/TiN composite coatings. Surf. Interface Anal. **43**, 1543–1548 (2011)
15. Selvan, J.S.; Subramanian, K.; Nath, A.K.; Kumar, H.; Ramachandra, C.; Ravindranathan, S.P.: Laser boronising of Ti–6Al–4V as a result of laser alloying with pre-placed BN. Mater. Sci. Eng. A **260**, 178–187 (1999)
16. ASTM G133-05: Standard Test Method for Linearly Reciprocating Ball-on-Flat Sliding Wear. ASTM International, West Conshohocken, PA (2016)
17. Sobiyi, K.; Akinlabi, E.: Microstructural investigation of laser cladded Ti on Ti6Al4 V. Mater. Today Proc. **4**, 244–249 (2017)
18. Song, J.L.; Li, J.T.; Deng, Q.L.; Cheng, Z.Y.; Chin, B.: Cracking mechanism of laser cladding rapid manufacturing 316 L stainless steel. Key Eng. Mater. **420**, 413–416 (2010)
19. Guo, C.; Zhou, J.S.; Zhao, J.R.; Chen, J.M.: Improvement of the tribological properties of pure Ti by laser cladding intermetallic compound composite coating. Proc. Inst. Mech. Eng. Part J: J. Eng. Tribol. **225**, 864–874 (2011)
20. Erinosho, M.F.; Akinlabi, E.T.; Pityana, S.: Influence of processing parameters on laser metal deposited copper and titanium alloy composites. Trans. Nonferrous Met. Soc. China **25**, 2608–2616 (2015)
21. Guo, C.; Zhou, J.; Chen, J.; Zhao, J.; Yu, Y.; Zhou, H.: Improvement of the oxidation and wear resistance of pure Ti by laser cladding at elevated temperature. Surf. Coat. Technol. **205**, 2142–2151 (2010)
22. Li, C.X.; Xia, J.; Dong, H.: Sliding wear of TiAl intermetallics against steel and ceramics of Al_2O_3, Si_3N_4 and WC/Co. Wear **261**, 693–701 (2006)
23. Ge, S.; Wang, S.; Gitis, N.; Vinogradov, M.; Xiao, J.: Wear behavior and wear debris distribution of UHMWPE against Si_3N_4 ball in bi-directional sliding. Wear **264**, 571–578 (2008)
24. Man, H.C.; Zhang, S.; Cheng, F.T.; Guo, X.: In situ formation of a TiN/Ti metal matrix composite gradient coating on NiTi by laser cladding and nitriding. Surf. Coat. Technol. **200**, 4961–4966 (2006)